Statistical analysis of the mesospheric inversion layers over two symmetrical tropical sites: Réunion (20.8° S, 55.5° E) and Mauna Loa (19.5° N, 155.6° W)

Nelson Bègue, Nkanyiso Mbatha, Hassan Bencherif, René Tato Loua, Venkataraman Sivakumar, Thierry Leblanc

Ann. Geophys., 35, 1177–1194, 2017
https://doi.org/10.5194/angeo-35-1177-2017

Annales Geophysicae
Open Access
EGU

Statistical analysis of the mesospheric inversion layers over two symmetrical tropical sites: Réunion (20.8° S, 55.5° E) and Mauna Loa (19.5° N, 155.6° W)

Nelson Bègue[1], Nkanyiso Mbatha[2], Hassan Bencherif[1,4], René Tato Loua[1,3], Venkataraman Sivakumar[4], and Thierry Leblanc[5]

[1]Laboratoire de l'Atmosphère et des Cyclones, UMR 8105 CNRS, Université de la Réunion, Météo-France, Réunion, France
[2]University of ZuluLand, Department of Geography, KwaDlangezwa, 3886, South Africa
[3]Centre de Recherche Scientifique de Conakry Rogbane, Conakry, Guinea
[4]School of Chemistry and Physics, University of KwaZulu Natal, Durban, South Africa
[5]California Institute of Technology, Jet Propulsion Laboratory, Wrightwood, CA 92397, USA

Correspondence to: Nelson Bègue (nelson.begue@univ-reunion.fr)

Received: 2 May 2017 – Revised: 15 August 2017 – Accepted: 25 September 2017 – Published: 2 November 2017

Abstract. In this investigation a statistical analysis of the characteristics of mesospheric inversion layers (MILs) over tropical regions is presented. This study involves the analysis of 16 years of lidar observations recorded at Réunion (20.8° S, 55.5° E) and 21 years of lidar observations recorded at Mauna Loa (19.5° N, 155.6° W) together with SABER observations at these two locations. MILs appear in 10 and 9.3 % of the observed temperature profiles recorded by Rayleigh lidar at Réunion and Mauna Loa, respectively. The parameters defining MILs show a semi-annual cycle over the two selected sites with maxima occurring near the equinoxes and minima occurring during the solstices. Over both sites, the maximum mean amplitude is observed in April and October, and this corresponds to a value greater than 35 K. According to lidar observations, the maximum and minimum mean of the base height ranged from 79 to 80.5 km and from 76 to 77.5 km, respectively. The MILs at Réunion appear on average ∼ 1 km thinner and ∼ 1 km lower, with an amplitude of ∼ 2 K higher than Mauna Loa. Generally, the statistical results for these two tropical locations as presented in this investigation are in fairly good agreement with previous studies. When compared to lidar measurements, on average SABER observations show MILs with greater amplitude, thickness and base altitudes of 4 K, 0.75 and 1.1 km, respectively. Taking into account the temperature error by SABER in the mesosphere, it can therefore be concluded that the measurements obtained from lidar and SABER observations are in significant agreement. The frequency spectrum analysis based on the lidar profiles and the 60-day averaged profile from SABER confirms the presence of the semi-annual oscillation where the magnitude maximum is found to coincide with the height range of the temperature inversion zone. This connection between increases in the semi-annual component close to the inversion zone is in agreement with most previously reported studies over tropics based on satellite observations. Results presented in this study confirm through the use of the ground-based Rayleigh lidar at Réunion and Mauna Loa that the semi-annual oscillation contributes to the formation of MILs over the tropical region.

Keywords. Meteorology and atmospheric dynamics (middle atmosphere dynamics)

1 Introduction

The thermal structure of the middle atmosphere cannot only be explained by radiative balance (Shepherd, 2000, 2007; Hauchecorne et al., 2010). The thermal properties of the mesosphere are determined by the dynamics of the atmosphere which results in the transport of air masses and momentum from the troposphere up to the mesosphere. As a consequence, this transport may lead to the formation of mesospheric temperature inversion layers (MILs). The term

inversion layer was given to this phenomenon because its appearance was similar to that of the inversion layer seen in tropospheric temperature profiles near the ground (Meriwether and Gerrard, 2004). MILs therefore refer to the temperature gradient inversion located in the mesosphere which was reported for the first time by Schmidlin (1976). Through the inter-comparison of data obtained by five different temperature measurement techniques in which the same MIL feature was found, Schmidlin (1976) demonstrated that MILs are not a phenomenon resulting from instrument error. It is now well recognized that MILs are a real geophysical phenomenon and the study of MILs is important for a comprehensive understanding of the structure and dynamics of the middle and upper atmosphere (Meriwether and Gardner, 2000; Meriwether and Gerrard, 2004). Meriwether and Gerrard (2004) reported that the understanding of the MILs is useful for the analysis of the stability and energy transfer in the middle and upper atmosphere. The positive temperature gradient observed at the base of the MILs (where the temperature begins to increase with increasing altitude) implies an increase in the atmosphere stability and reduction of vertical mixing. On the other hand, the negative temperature gradient located at the topside of the MILs (where the temperature begins to decrease with increasing altitude) implies a reduction in the atmospheric stability, which could induce convective instability (Meriwether and Gerrard, 2004). Moreover, MILs are mainly linked to the propagation of gravity waves which have a crucial impact on the dynamic and thermal structure in the middle and upper atmosphere (Dewan and Picard, 2001). Indeed, it is well known that wave breaking represents the primary means by which energy is transferred in the upper atmosphere. MILs may be divided into two subtypes, namely lower and upper MILs, which occur at approximately 75 and 95 km, respectively (Meriwether and Gardner, 2000; Meriwether and Gerrard, 2004). The upper MILs are formed when a strong tidal wave non-linearly interacts with gravity waves propagating from below. Liu et al. (2000) showed that breaking gravity waves can warm the air sufficiently for the formation of MILs if the static stability of the mesosphere had been decreased by a tidal wave. Models and observations have revealed that the upper MILs have an amplitude maximum during the winter at mid-latitudes (Dao et al., 1995; Liu et al., 2000; Meriwether et al., 1998). The occurrence of the lower MILs is a characteristic and persistent feature of the winter mesosphere and lower thermosphere (MLT) (Hauchecorne et al., 1987; Meriwether and Gardner, 2000). Hauchecorne et al. (1987) reported that MILs are larger in winter than in summer, while their mean heights are lower in winter than in summer at mid-latitudes. Moreover, the lower MILs could occur with amplitudes greater than 30 K and are observed more than 20 % of the time, whereas the amplitude of the upper MILs range from 10 to 30 K (Meriwether and Gardner, 2000). It is worth noting that it is not yet understood whether the lower and upper MILs occur through the same mechanisms. This investigation focuses exclusively on lower MILs and throughout this article the term MIL will be used to refer to lower MILs.

The characteristics of MILs have been investigated using various instruments including ground-based Rayleigh lidar (Hauchecorne et al., 1987; Meriwether et al., 1998; Whiteway et al., 1995; Siva Kumar et al., 2001; Ratnam et al., 2003), sodium temperature lidar (She et al., 1993; States and Gardner, 2000) and satellites (Clancy and Rusch, 1989; Clancy et al., 1994; Leblanc and Hauchecorne, 1997; Fadnavis and Beig, 2004; Fechine et al., 2008; Gan et al., 2012; Szewczyk et al., 2013). Satellite measurements have greatly contributed to the knowledge of latitudinal variations in MILs. Different satellite instruments show good agreement between one another and reveal that MILs exhibit an apparent latitudinal dependence. Based on 7 years of SABER (Sounding of the Atmosphere using Broadband Emission Radiometry) observations on board the TIMED (Thermosphere, Ionosphere, Mesosphere Energetics and Dynamics) satellite, Gan et al. (2012) showed that MILs at low latitudes exhibit a semi-annual cycle and reach their maximum amplitude (30–40 K) in spring and autumn. By comparison, at middle latitudes an annual cycle appears with the maximum amplitude (24–33 K) observed in winter. Furthermore, it was found that the frequency of MILs reached a maximum value of 90 % during equinox in equatorial and tropical regions, whereas a maximum of 70 % was observed in winter at middle and high latitudes. Combining ground-based Rayleigh lidar observations, ISAMS (Improved Stratospheric And Mesospheric Sounder) and HALOE (Halogen Occultation Experiment) temperature measurements from UARS (Upper Atmospheric Research Satellite) observations, Leblanc and Hauchecorne (1997) proposed a detailed climatology of MILs. They found that the latitudinal variations are largely symmetric about the Equator. Ground-based Rayleigh lidar observations are very helpful to understand the MIL morphology with good vertical resolution, particularly at mid-latitudes. In particular, studies reported in the literature regarding MILs detected by ground-based Rayleigh lidar are principally realized for this latitude region (Hauchecorne et al., 1987; Whiteway et al., 1995; Leblanc and Hauchecorne, 1997; Meriwether et al., 1998; States and Gardner, 1998; Duck et al., 2001). A further reason for studies being carried out in this specific latitude range is that most of the ground-based Rayleigh lidar facilities are located at mid-latitudes (Gan et al., 2012). As a direct result, investigations using ground-based Rayleigh lidar at tropical latitudes are very sparse. The few studies reported in the literature using this measurement technique at tropical regions were mainly carried out at Gadanki (13.5° N, 79.2° E) (Siva Kumar et al., 2001; Nee et al., 2002; Ratnam et al., 2002, 2003; Kishore Kumar et al., 2008). Based on analysis of 4 years of temperature profiles recorded at Gadanki, Ratnam et al. (2003) found that the characteristics of MILs over this tropical site evolve in time following an annual cycle, with a maximum occurring during summer and a corresponding minimum in

winter. Using 8 years of lidar observations, Kishore Kumar et al. (2008) found a clear semi-annual cycle in the MIL occurrence at the Gadanki site.

Although MILs are frequently observed on mesospheric temperature profiles from the Equator to high latitudes, a possible formation mechanism is not well established (Meriwether and Gerrard, 2004). Several MIL formation mechanisms involving wave activity have been proposed and are well documented by Meriwether and Gerrard (2004). Based on Rayleigh lidar observations, Hauchecorne et al. (1987) proposed that the inversion observed near 75 km at middle latitudes is linked to gravity wave breaking. In this scenario gravity waves propagating into higher altitudes deposit their momentum thereby decelerating the local wind. The breaking of these waves then produces turbulence inside and above the inversion layer (Hauchecorne et al., 1987; Whiteway et al., 1995; Ratnam et al., 2002). However, some studies indicate that the breaking of gravity waves is not strong enough to produce a high amplitude value of 35–40 K (Fritts and van Zandt, 1993; Lubken, 1997; Ratnam et al., 2003). Based on rocket sounding performed between 1991 and 1997, Lubken (1997) showed that wave dissipation provides a maximum heating rate of about 10–20 K day^{-1} during summer. Through the use of Rayleigh lidar observations at Utah (41.7° N, 111.8° W), Meriwether et al. (1998) provided evidence to support the assumption that MILs result from the interaction between gravity wave with tidal structures. The analysis of the Rayleigh lidar observations at Eureka (80° N, 86° W) reveals a distribution with altitude similar to that found at middle latitudes but without a relationship to stratospheric gravity wave activity (Duck and Greene, 2004). Satellite observations have also contributed to improving the understanding of MIL characteristics. More recently, through the analysis of monthly zonal mean temperature data obtained from SABER observations, Gan et al. (2012) suggested that semi-annual oscillations are the fundamental cause of large spatio-temporal-scale MILs at low latitudes. Parallel to observations, numerical modelling of temperature inversion layers has also contributed significantly to the understanding of this phenomenon. An alternative formation mechanism was presented by Meriwether and Mlynczak (1995) using a two-dimensional model. This combined a comprehensive model of mesosphere photochemistry with dynamic transport of long lived species. This study suggested that MILs are due to chemical heating through exothermic reactions (implying the presence and chemical involvement of ozone). However, Leblanc and Hauchecorne (1997) estimated that the heating rate produced by these reactions does not seem to be efficient enough for the development of inversions of amplitude such as 40 K, especially in the lower mesosphere and during the day. They suggested that a chemical source of temperature enhancement which resulted in a temperature inversion could be plausible only above 85 km. Various possible exothermic reaction involving O_x and HO_x were suggested as being responsible for the heating in the middle atmosphere during daytime (Berger and von Zahn, 1999). Using the Whole Atmosphere Community Climate model (WACCM) including a parameterization of both orographic wave and a spectrum of travelling gravity wave, Sassi et al. (2002) demonstrated that MIL events arise as a consequence of rapid wave-breaking dissipation of planetary waves at middle latitudes. More recently, France et al. (2015), also using the WACCM model, showed that MILs at middle latitudes are driven by decay of vertically propagating planetary waves in the mesospheric surf zone. Previous studies therefore suggest a latitudinal variation in the characteristics of the MILs with different possible formation mechanisms.

Because of a lack of ground-based observations over Southern Hemisphere tropical/subtropical latitudes, questions arise regarding the characteristics of MILs and their formation mechanisms in these regions. In this investigation, Rayleigh lidar data recorded at Réunion (20.8° S, 55.5° E) since 1994 and at Mauna Loa (19.5° N, 155.6° W) since 1993 have been employed. These data were recorded within the framework of the Network for the Detection of Atmospheric Composition Change (NDACC) (Keckhut et al., 2004). These lidar systems have been providing quasi-continuous temperature profiles in the altitude range 30 to 80 km. The Réunion Rayleigh lidar temperature measurements have already been used for case studies and climatological analysis of the middle atmosphere (Morel et al., 2002; Moogawa et al., 2007; Batista et al., 2009; Raju et al., 2010; Sharma et al., 2017). Based on Rayleigh lidar observations at Réunion from October to November 1995, Morel et al. (2002) analysed the tidal perturbation on the temperature profiles. Sivakumar et al. (2011) proposed a climatology of stratosphere-mesosphere temperature from 14 years of Rayleigh lidar data recorded at Réunion. They found a predominant semi-annual oscillation between 30 and 60 km with a maximum temperature at the equinoxes and a minimum at the solstices. The Rayleigh lidar located at Mauna Loa constitutes a unique and valuable dataset to study the long-term middle atmospheric temperature and dynamical variability in the tropical/subtropical region in the Northern Hemisphere (Leblanc et al., 1998, 1999; Leblanc and McDermid, 2001; Li et al., 2008, 2010; Dou et al., 2009). Leblanc et al. (1998) completed a climatological study of middle atmosphere temperature including lidar observations recorded at Mauna Loa during the period 1993–1997. They found that the amplitude of the seasonal temperature variation is weak and characterized by a clear semi-annual oscillation. It is worth noting that, to date, no study on MILs using Rayleigh lidar observations at Réunion has been published.

In this investigation, 16 and 21 years of Rayleigh lidar observations collected at Réunion and Mauna Loa, respectively, have been employed to produce a statistical analysis of the characteristics of the MILs and to determine their seasonal variability. The Mauna Loa and Réunion lidar systems have been providing quasi-continuous temperature pro-

files in the 12–90 and 30–80 km altitude ranges, respectively. These lidar results will be compared to those obtained from SABER observations where relevant. This paper is organized as follows. Section 2 describes the data and the method used to detect MILs. Section 3 provides results of the statistical analysis obtained from Rayleigh lidar observations. Section 4 presents the intra- and inter-annual variability of MILs. The similarity of MIL characteristics between these two sites (symmetrical about the Equator) is discussed in Sect. 5. A summary and conclusions are presented in Sect. 6.

2 Data and methodology

2.1 Observations

2.1.1 Ground-based Rayleigh lidar observations

The ground-based Rayleigh lidar temperature profiles employed in this study were recorded at Réunion (20.8° S, 55.5° E) since 1994 and Mauna Loa (19° N, 155° W) since 1993 within the framework of NDACC network. The two Rayleigh lidar temperature datasets were downloaded from the NDACC website (http://www.ndsc.ncep.noaa.gov/). The lidar systems at Réunion and Mauna Loa are described in detail by Bencherif et al. (1996) and McDermid et al. (1995), respectively. The Rayleigh–Raman lidar system at Mauna Loa was established by the Jet Propulsion Laboratory (JPL) and has been in operation since 1993. Between 1993 and 2001, the emitter system consisted of an excimer laser beam at 308 nm shifted through a nitrogen Raman cell to transmit 353 nm, at a repetition rate of 200 Hz. In 2001, it was replaced by a Nd:YAG laser (1064 nm), tripled to transmit at 355 nm with a repetition rate of 50 Hz. The optical receiver includes a Cassegrain telescope (0.91 m diameter) coupled with a six-channel polychromator, three of those channels being used for temperature retrieval (two 353/355 nm Rayleigh backscatter channels and one 385/387 nm vibrational Raman backscatter channel). The signals collected by the photomultipliers are sampled by multi-channel scalers (MCS) at 2 µs intervals (300 m) and saved in the raw data files every 5 to 20 min, depending on the period considered over the 1993–present time series. During processing, the temperature profiles are further integrated to a 2 h average and then vertically smoothed to yield an effective resolution ranging from 300 m in lower stratosphere to 4 km in the upper mesosphere, following the NDACC-standardized definition detailed in Leblanc et al. (2016a). Temperature uncertainty ranges from 0.5 K in the mid-stratosphere to 2 K in the lower mesosphere, and more than 10 K in the upper mesosphere as a result of lower signal-to-noise ratios and uncertainty owing to the "a priori" temperature initialization. A full uncertainty budget for Rayleigh/Raman temperature lidars with a specific example for the Mauna Loa system is presented in Leblanc et al. (2016b). At Réunion, the Rayleigh lidar system was established at the Saint-Denis campus (approximately sea level) by the Laboratoire de l'Atmosphere et des Cyclones (LACy) and was operational from 1994 to 2009. The lidar temperature profiles at Réunion were recorded with the use of a Nd:YAG laser (emitting at 532 nm). The laser is operated at 30 Hz with corresponding pulse energy of 300 mJ. Backscattered photons are collected by a telescope composed of four mirrors with a total surface area of 0.67 m^2. The lidar return signal is collected with a height resolution of 300 m and time integration of 122 s.

Temperature profiles from the Rayleigh lidar measurements are derived according to the analytical method used by Chanin and Hauchecorne (1984). In the altitude range where Mie scattering is negligible ($\sim$ 30–80 km) and assuming that the atmosphere is in hydrostatic equilibrium, the recorded signal intensity is proportional to the molecular number density. At the top of the atmosphere ($\sim$ 80 km), where the signal-to-noise ratio is fairly high, the COSPAR International Reference Atmosphere (CIRA-86) standard model (Rees et al., 1990; Barnett and Corney, 1985) and MSISE-00 (Hedin, 1991) model are used as a reference pressure value at Réunion and Mauna Loa, respectively. The vertical temperature profile is then computed downward using the measured density profiles and the computed pressure profile initialized by the CIRA and MSISE-00 model at Réunion and Mauna Loa, respectively. Leblanc et al. (1998) showed that the uncertainty at the top of the profile decreases rapidly and an uncertainty of 15 % in the pressure corresponds to a temperature uncertainty less than 2 %. Kishore et al. (2014) reported that in individual profiles, the temperature accuracy varies between 0.5 and 1.5 K in the stratosphere and 2 and 3 K in mesosphere.

The Réunion lidar dataset contains 1321 temperature profiles recorded quasi-continuously from May 1994 to August 2009. It should be noted that no temperature profiles were recorded at Réunion during 2007 because of laser technical problems. At the Mauna Loa site, 21 years (October 1993–April 2014) of continuous Rayleigh lidar observations were used. This dataset corresponds to a total of 2526 temperature profiles. The total number of profiles per year and for both sites ranges between 39 and 140. On average this is equivalent to approximately 30 temperature profiles per month. Réunion and Mauna Loa temperature lidar profiles have been widely used in different research projects (Leblanc et al., 1998, 1999; Morel et al., 2002; Cadet et al., 2003; Bencherif et al., 2007; Dou et al., 2009; Sivakumar et al., 2011; Kishore et al., 2014).

Due to the initialization of the pressure at the top of the profile by an atmospheric model (CIRA-86; MSISE-00), the uncertainty in the temperature values in the mesosphere (at altitudes above 80 km) is the highest. Since upper MILs are usually situated at an average altitude greater than 85 km, this study will focus on the investigation of lower MILs which are usually located below 82 km (Meriwether and Gerrard, 2004).

2.1.2 SABER observations

This study employed vertical temperature profiles level 2A data measured by the Sounding of the Atmosphere using Broadband Emission (SABER) instrument, which is one of the four instruments on board the Thermosphere, Ionosphere, Mesosphere, Energetics and Dynamics (TIMED) satellite. These data can be downloaded from the web site http://saber.gats-inc.com. This instrument (SABER) primarily assists in providing understanding of the thermal structure of the stratosphere, mesosphere and the lower thermosphere (Remsberg et al., 2003). The TIMED satellite was launched on 7 December 2001, and it operates in nadir view from its 625 km circular orbit at a 74.1 inclination angle with a period of about 102 min (Russell III et al., 1999; Remsberg et al., 2003). The SABER instrument started taking measurements in late January 2002, and it continues to provide global coverage of atmospheric thermal structure giving profiles from 52° S and 83° N during which time it is in its northwards-looking mode (for approximately 2 months) before switching to southwards-looking mode, where it repeats the same sequence for another 2 months (Remsberg et al., 2003). The SABER vertical profiles are produced every 52 s, with a profile spacing of approximately 3° of latitude for every 15 orbits per day, and with each profile having a vertical resolution of $\sim$ 2 km.

The SABER kinetic temperature profiles have accuracies of the measurements which are 1.5 K for 15–80 km and 4 K for 80–100 km. More details regarding errors in SABER kinetic temperature especially due to non-local thermodynamic equilibrium (non-LTE) model parameters are explained by a study by Garcia-Comas et al. (2008). This is primary because non-LTE effects are said to be dominant at higher altitudes, especially of the extratropics of the upper mesosphere (Mertens et al., 2004; Remsberg et al., 2003). In this study, we chose to use a level 2 SABER data product which included significant improvement to temperature algorithm such as the procedure to retrieve temperature for conditions that are not in local thermodynamic equilibrium (nLTE). The technical details of these datasets are described in the SABER Algorithm Document, available at http://saber.gats-inc.com/documentation.php. In this investigation, 13 years (February 2002–February 2015) of SABER overpasses (within ±5° in latitudinal and longitude shift) for the two selected lidar locations, Réunion and Mauna Loa, were employed. This surface area was chosen to guarantee at least 10 satellite profiles per day. Taking into account the conditions mentioned previously, 17 550 and 17 553 temperature profiles were used over Réunion and Mauna Loa, respectively. The valuable nature of SABER observations for the study of the middle atmosphere is well documented in previous research (Meriwether and Gerrard, 2004; Fechine et al., 2008; Dou et al., 2009; Gan et al., 2012; France et al., 2015).

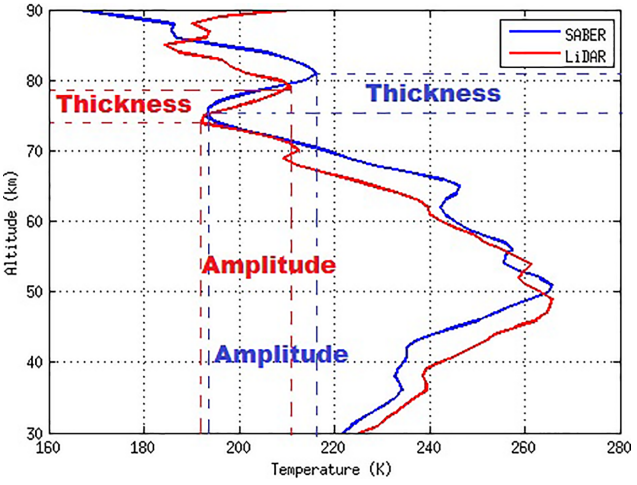

Figure 1. Vertical temperature profile obtained from lidar (red line) and SABER (blue line) measurements over Réunion on 13 June 2005. The thickness (lidar = 5.2 km; SABER = 6.1 km) and the amplitude (lidar = 18.5 K; SABER = 23.3 K) of the MIL are indicated by the dashed line.

2.2 Detection and analysis of the MILs (methodology)

MILs were identified by following the procedure outlined by Leblanc and Hauchecorne (1997) and Fechine et al. (2008) and which is briefly presented here. It is worth noting that this procedure has been applied in many previous studies investigating the phenomenon of mesospheric inversion (Leblanc et al., 1998; Meriwether and Gardner, 2000; Duck et al., 2001; Duck and Greene, 2004; Cutler et al., 2001; Siva Kumar et al., 2001; Ratnam et al., 2003; Gan et al., 2012). Figure 1 shows an example of a vertical temperature profile obtained from lidar and SABER observations over the Réunion site and showing a significant MIL structure. The identification procedure of Leblanc and Hauchecorne (1997) is based on the characteristics of the temperature inversion. In particular, the thickness and the amplitude which correspond to differences in altitude and temperature between the top and bottom level of the inversion layers, respectively (see Fig. 1). MILs are identified by using the following three criteria: (1) the bottom of the inversion is located at least 5 km above the stratopause and the top is below 90 km, (2) the amplitude is larger than 10 K and (3) the thickness is greater than or equal to 4 km. The temperature inversions which satisfy the above mentioned criteria are considered as significant MILs. It is to be noted that this MIL diagnostic was applied on the daily lidar and SABER profiles.

Once all temperature profiles with significant MIL structures have been identified, a descriptive statistical analysis is performed. In the descriptive statistical analysis, basic statistical parameters and distribution functions are produced from the derived inversion dataset. A difference in the characteristics of the MILs such as frequency between the two sites is

judged significant when the frequency of one sample is not within the confidence interval of the other sample (Wilks, 1995).

3 Statistical analysis of temperature inversion layer

The application of the methodology described above to Rayleigh lidar observations (1994–2009) shows that a total of 132 and 210 MIL events are detected over Réunion and Mauna Loa, respectively. These MIL occurrences correspond to 10 and 8.3 % of temperature profiles at Réunion and Mauna Loa, respectively. Taking into account the whole lidar dataset of observations over Mauna Loa (1993 to 2014), the frequency of MIL occurrence is slightly higher and represents 9.3 % of the total profiles recorded. From the statistical results obtained during the same period, it is clear that MILs are slightly more frequent over the Réunion site. However, this result may be biased by the difference in temporal sampling between the two sites as presented in the previous section. Moreover, similar results are obtained using satellite observations which have at least one profile per day, per site. From satellite temperature profiles, occurrence rates of 19 and 15 % over Réunion and Mauna Loa are observed, respectively.

Figure 2 illustrates the monthly evolution of MIL occurrence rates over Réunion and Mauna Loa. In agreement with the previous comments, Fig. 2 shows that generally the monthly frequency of detection of MILs at Réunion is slightly higher than at Mauna Loa, particularly from satellite observations. According to SABER observations, the maximum occurrence rate over Mauna Loa is obtained in April (12 %) and October (14 %), near the equinoxes, whereas the minimum is observed during January (8 %) and September (6 %), near the solstice (Fig. 2a). Based on SABER observations, the maxima in MIL occurrences over Réunion are observed in April (16 %) and November (18 %), near the equinoxes, whereas the minima are observed with SABER during February (6 %) and August (11 %), near the solstice. The lidar observations over Mauna Loa confirm the same seasonal variation with a maximum in occurrence rate corresponding to the equinoxes and the minimum corresponding to the solstice (Fig. 2a). The results obtained over Réunion are in fairly good agreement with those obtained over Mauna Loa. Nevertheless, it can be observed that the lidar observations over Mauna Loa show slightly different behaviour mainly during the winter months (Fig. 2a). The reason could be the gravity wave activity, which is much stronger in the Northern Hemisphere middle atmosphere compared to the Southern Hemisphere. It is important to note that lidars are very sensitive in detecting gravity wave activity in the atmosphere. The wave activity (including gravity waves) in the middle atmosphere is primarily of tropospheric origin. Topography plays an important role in initiating these waves, and they grow with amplitude as they propagate upwards.

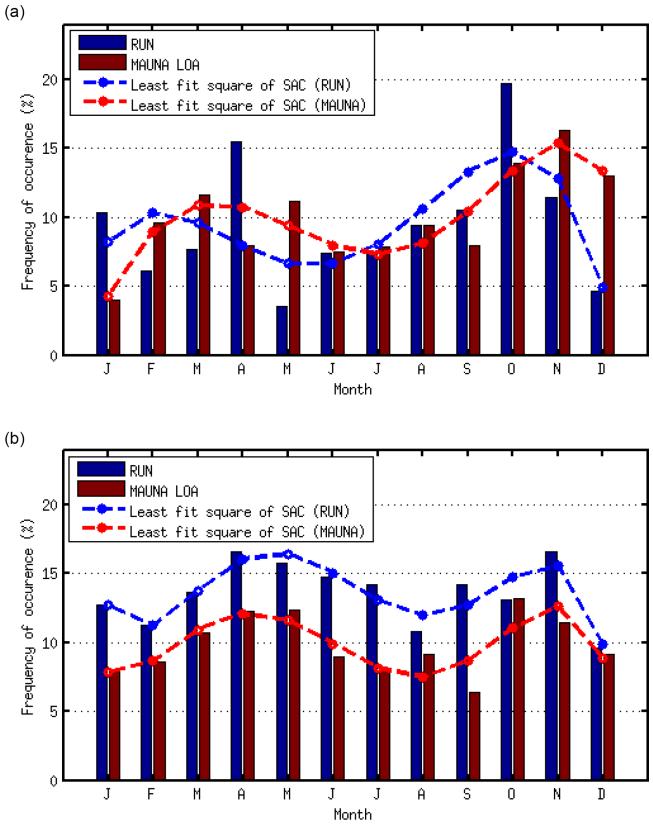

Figure 2. Frequency of occurrence of MIL events over Réunion (blue) and Mauna Loa (red) obtained from **(a)** lidar during the 1994–2009 period and **(b)** SABER observations during the 2002–2015 period. The red and blue curves correspond to least squares fit of semi-annual oscillation for Mauna Loa and Réunion, respectively.

The Southern Hemisphere and Northern Hemisphere have varying and diverse geophysical processes due, for example, to the difference in land cover, ocean size and radiation fluxes. In relation to the generation of gravity waves in the troposphere, the Southern Hemisphere is dominated by the ocean (hence inducing less gravity wave activity), whereas the Northern Hemisphere is dominated by land cover (hence inducing more gravity wave activity). Studies such as Fritts and Vanzandt (1993) and Fritts and Alexander (2003) have showed significant differences between the Southern Hemisphere and the Northern Hemisphere with regard to gravity wave activity in the middle atmosphere, primarily due to topography differences. These results are in agreement with previous studies (Leblanc and Hauchecorne, 1997; Siva Kumar et al., 2001; Fechine et al., 2008) and are discussed more fully in Sect. 5.

The monthly evolution obtained from ground-based and satellite observations reveals a semi-annual modulation at both sites. This is best illustrated by the least squares fits representing the semi-annual cycle and is superimposed in Fig. 2a and b. The least squares fit plots illustrate how the

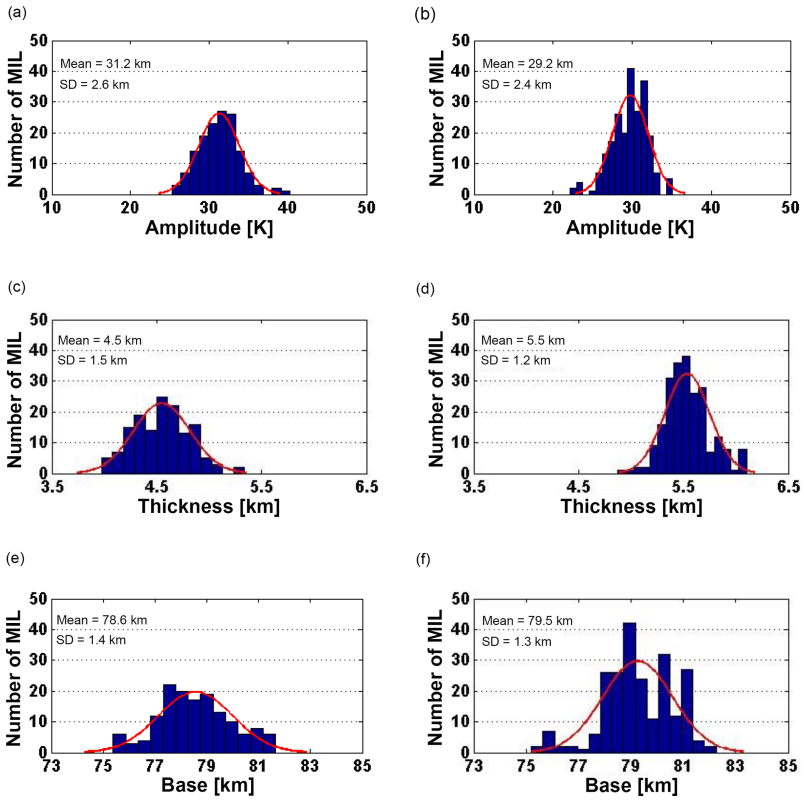

Figure 3. Distribution of MIL **(a, b)** amplitude, **(c, d)** thickness and **(e, f)** base over Réunion **(a, c, e)** and Mauna Loa **(b, d, f)** from lidar observations during the 1994–2009 period and the 1994–2014 period, respectively.

MIL occurrence rates are driven by the semi-annual forcing, with root mean square difference (RMSD) of the order of 1.6 relative to the annual cycle and with an RMSD of the order of 5.2. Consideration of Fig. 2b shows that the semi-annual cycle is well defined in SABER temperature profiles. This could be due to the fact that the temporal sampling is better from satellite observations than from lidar measurements. It should be noted that the semi-annual cycles obtained from SABER observations over both sites are in phase, whereas a delay of 1 month is observed in lidar observations (see Fig. 2). Based on satellite observations, Leblanc and Hauchecorne (1997) showed that the evolution of MIL occurrence rates at lower latitude follows a semi-annual cycle with the maximum near the equinoxes. More recently, by using SABER observations over Cariri (Brazil; 7.4° S, 36.5° W) during 2005, Fechine et al. (2008) showed that the maximum occurrence of MILs occurred in April and October, whereas the minimum occurred in January and July. Over two symmetrical tropical sites they demonstrated that the monthly evolution of the frequency of occurrence of MILs is similar and shows a dependency on the solstices and equinoxes.

It is worth noting that this investigation shows a significant difference between the two selected sites in January. The occurrence rate of the lower MILs in January is around 2 times higher over Réunion than Mauna Loa (see Fig. 2a). In January, MILs represent 10 % of the temperature profiles at the Réunion site. This may suggest that other processes could be involved during this period at this location. This observation could be related to the increase in convective activity in the southwestern Indian Ocean (SWIO) basin during this period. It is well known that low-pressure and tropical cyclone systems are a source of low-frequency convective gravity waves in the SWIO basin (Chane-Ming et al., 2007, 2010; Ibrahim et al., 2010). Based on a 10-season climatology investigation (1997/1998–2006/2007) obtained from GPS windsonde, Ibrahim et al. (2010) showed a linear relationship between weekly gravity waves total energy density in the lower stratosphere and the activity of intense tropical cyclones in the SWIO basin. These gravity waves which were produced through the activity of intense tropical cyclones could also influence the dynamics of the middle atmosphere as well as the general circulation.

Probability density function (PDF) parameters of MIL characteristics at Réunion and Mauna Loa are shown in Fig. 3 and summarized in Table 1. It is worth noting that the characteristics of the MILs are significantly distributed following a normal law. For both sites, MILs are found to be distributed to the altitude range 75 to 82 km with a maximum amplitude exceeding 30 K (see Fig. 3). It should also be noted that the statistical distribution presented in this work

Table 1. The inversion characteristics at Réunion and Mauna Loa from lidar. The inversion characteristics obtained from SABER are reported in parentheses. The confidence interval of the mean is calculated at 95% level.

	Amplitude (K)		Thickness (km)		Base (km)	
	Mauna Loa	Réunion	Mauna Loa	Réunion	Mauna Loa	Réunion
Mean	29.2 (33.6)	31.2 (34.8)	5.5 (5.9)	4.5 (5.6)	79.5 (80.5)	78.6 (79.8)
SD	2.4 (2.3)	2.6 (2.8)	1.2 (1.5)	1.5 (1.8)	1.3 (1.5)	1.4 (1.6)
CI	±0.3 (±0.3)	±0.4 (±0.5)	±0.2 (±0.4)	±0.3 (±0,3)	±0.2 (±0.3)	±0.2 (±0.2)

is fairly consistent with the work published by Siva Kumar et al. (2001) over Gadanki (13.5° N, 79.2° E). Based on 119 nights of Rayleigh lidar observations from March 1998 to February 2000, Siva Kumar et al. (2001) showed that the peak of the inversion layer is confined to the altitude range 73 to 79 km with a maximum at approximately 76 km. The analysis of the PDFs reveals that the mean values of MIL characteristics are quite different for the two sites. On average, the thickness and the base of the MILs at Mauna Loa are 1 km higher than at Réunion (Table 1). However, the amplitude of the MILs is on average higher over Réunion (31.2 K) than Mauna Loa (29.2 K). The confidence intervals of the mean are calculated at 95 % and indicate that the differences between the two sites are statistically significant (Table 1). At both sites, the inversion characteristics obtained from SABER observations are higher than those obtained from lidar observations (Table 1). The difference between SABER and lidar observations over both sites will be discussed in detail in the next section.

4 Intra- and inter-annual variability

Figure 4 depicts the time evolution of monthly average (a) amplitude, (b) thickness and (c) base of the temperature inversion layer obtained from lidar observations during 1994–2009 over Réunion (blue line) and during 1993–2014 over Mauna Loa (green line). The corresponding standard deviations are represented by the vertical bars. As expected, the amplitude of the MILs shows a semi-annual cycle over the two sites with maxima near the equinoxes and minima during the solstices. Over Réunion, the maximum mean amplitude reaches 32 ± 6 K during equinoxes, while the minimum mean amplitude is 28 ± 5 and 30 ± 5 K during summer and winter, respectively. Over Mauna Loa, the maximum and minimum are 30 ± 6 and 20 ± 6 K near equinoxes and solstices, respectively. The evolution of monthly averages of the MIL parameters obtained from SABER observations during 2002–2015 over Réunion (red line) and Mauna Loa (black line) is also shown in Fig. 4. On average the amplitude over Réunion is higher than Mauna Loa throughout the year, except during the September–October period particularly from satellite observations. Over both sites, the maximum mean amplitude obtained from SABER is observed in April and October and corresponds to a value greater than 35 K. Over the both sites, the first minimum amplitude is January. The second minimum is observed in June (30 ± 4 K) and September (30 ± 3 K) over Mauna Loa and Réunion, respectively.

Unlike the two mean parameters (amplitude and base of MIL events), the semi-annual cycle is not significant in the monthly evolution of MIL thickness obtained from both lidar and SABER measurements (see Fig. 4b). Thickness appears to be approximately constant during the first months of the year (February to April). The measurements of SABER MIL thickness seems to be greater over Mauna Loa than at Réunion. According to lidar observations, the monthly evolution of MIL thickness have a fairly similar shape for both sites and are at a quasi-constant difference of 1 km apart throughout the year (see Fig. 4b). The lidar observations reveal that maximum mean thicknesses are observed in May and November with average values of 4.8 ± 1.2 km and 5.6 ± 1.3 km over Réunion and Mauna Loa, respectively. As a whole, the time evolution of monthly average thickness of the MILs obtained from SABER and lidar observations at Réunion compare fairly well. However, consideration of Fig. 4b shows that the thickness obtained from SABER is higher than that measured by lidar. On average, for Réunion and Mauna Loa this difference between SABER and lidar measurements corresponds to a difference of approximately 1.1 and 0.4 km, respectively (Table 1). As reported by Leblanc and Hauchecorne (1997), the altitudes where these inversions occur are sources of uncertainty. This is because the tops of the inversions are close to critical altitude. As a result some inversions do not appear very significant because of poor accuracy of the measurements. When compared to the two previous parameters, the magnitude of the semi-annual cycle is more significant in the evolution of the height of the base (Fig. 4c). Furthermore, the monthly evolution obtained from the lidar and SABER observations is fairly similar, particularly in the first 5 months of the year. It is therefore clearly seen that the height of the base is at a maximum near the equinoxes and a minimum during the solstice. Moreover, the Mauna Loa lidar does show a maximum during January, especially in both the amplitude and thickness. It is a well-known fact that January and February of the Northern Hemisphere may have a major stratospheric sudden warming (SSW) at least every 2 years. During such an event, planetary waves tend to slow down the mean flow in the middle atmosphere, which induces a suitable en-

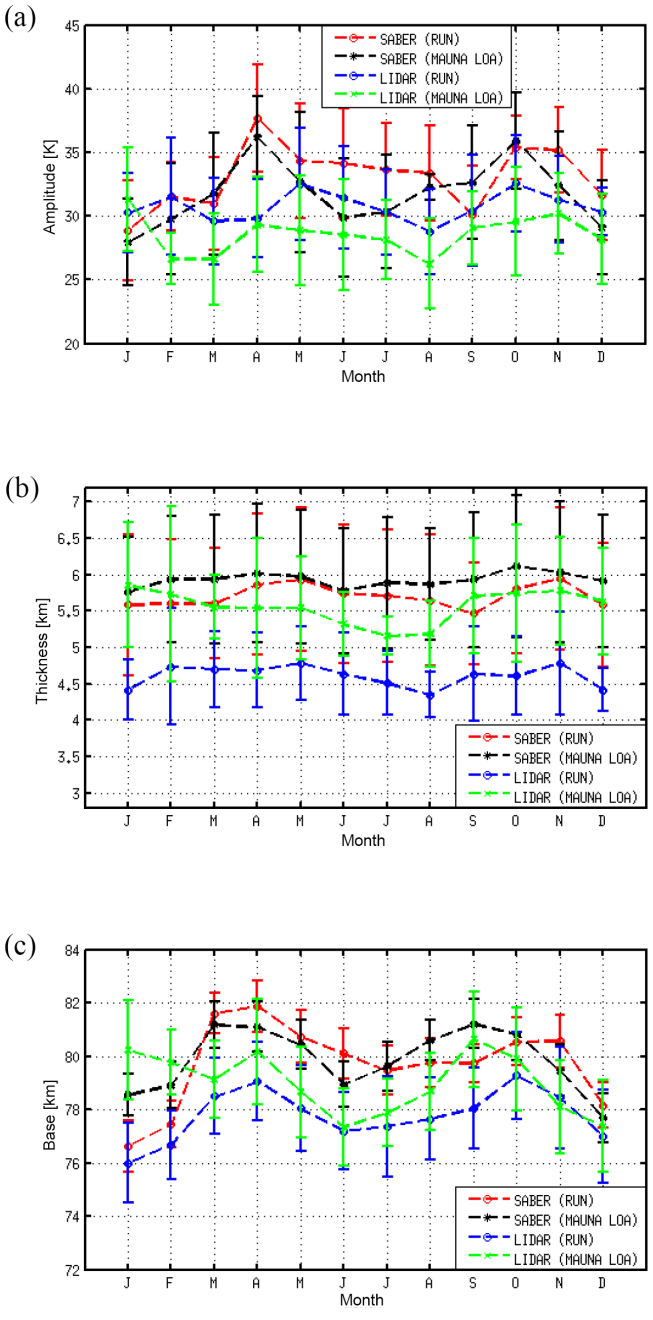

Figure 4. Time evolution of monthly averaged **(a)** amplitude, **(b)** thickness and **(c)** base of the inversion layer obtained from lidar and SABER observations during 1994–2009 over Réunion (red line) and during 1993–2015 over Mauna Loa (black line).

vironment for gravity waves to propagate all the way upward to the mesosphere–lower thermosphere region. Usually, the planetary wave activity becomes stronger just before a major SSW (Dawdy et al., 2004; Hoffmann et al., 2007; Mbatha et al., 2010). Previous studies have shown that the increase in planetary waves (France et al., 2015) and gravity waves (Hauchecorne et al., 1987) in the middle atmosphere creates good conditions for MILs to take place. Lidar is capable of detecting fluctuations of gravity waves scales, while these could be filtered out in satellite observations. Therefore, it may not be surprising that the maximum occurrence of MILs is observed in January. One case study which reported similar behaviour is a study by Irving et al. (2014). The seasonal behaviour of height of the base is opposite to that of amplitude and thickness in that the difference between the two sites obtained from the lidar and SABER observations concerning the height of the base is fairly similar ($\sim$ 1.1 km on average). According to lidar observations, the maximum and minimum mean of the base height range from 79 to 80.5 km and from 76 to 77.5 km, respectively. The interval of the maximum and minimum mean of the base altitudes obtained from SABER observations is slightly higher with values ranging from 80.5 to 82 km and from 77 to 79 km, respectively. The observations of MILs at Réunion and Mauna Loa are in quite good agreement with those reported previously (Leblanc et Hauchecorne, 1997; Fadnavis and Beig, 2004; Fechine et al., 2008; Ratnam et al., 2002, 2003; Siva Kumar et al., 2001; Gan et al., 2012). A detailed discussion and comparison of the results obtained in this study with results from previous studies over tropical regions is given in Sect. 5.

Figure 5 shows the time evolution of monthly amplitude, thickness and base height plotted for both SABER and lidar (Réunion and Mauna Loa) for the period from early 2002 for the SABER observations and 1993 and 1994 for Mauna Loa and Réunion lidar data, respectively. It is apparent that the SABER satellite observations reveal higher values than lidar over both sites, for the three parameters: amplitude, thickness and base height of MIL events.

The amplitude of the MILs as observed by SABER data varies between 27 and 40 K for both Réunion and Mauna Loa sites, while by comparison both lidar datasets indicate that the amplitude of the MILs varies between 23 and 32 K. The monthly mean of MILs as measured by SABER seems to indicate two peaks of the amplitude ($\sim$ 40 K) during the 2011–2012 period over the Réunion site (see Fig. 5a). The monthly amplitude means of MILs as measured by SABER seems to indicate an upwards trend for both the Southern Hemisphere and the Northern Hemisphere respectively, while this is not apparent for other parameters. However, for some periods it is possible to observe a decrease in the magnitude of the thickness and base evolutions (see Fig. 5b and c). For instance, a decrease in the magnitude of the thickness variations is observed during the period 2004–2007.

In spite of the many studies being carried out, the parameters governing the variability of MILs are not fully understood. The possible parameters involved in the behaviours of MILs for these two locations will be discussed in the next section.

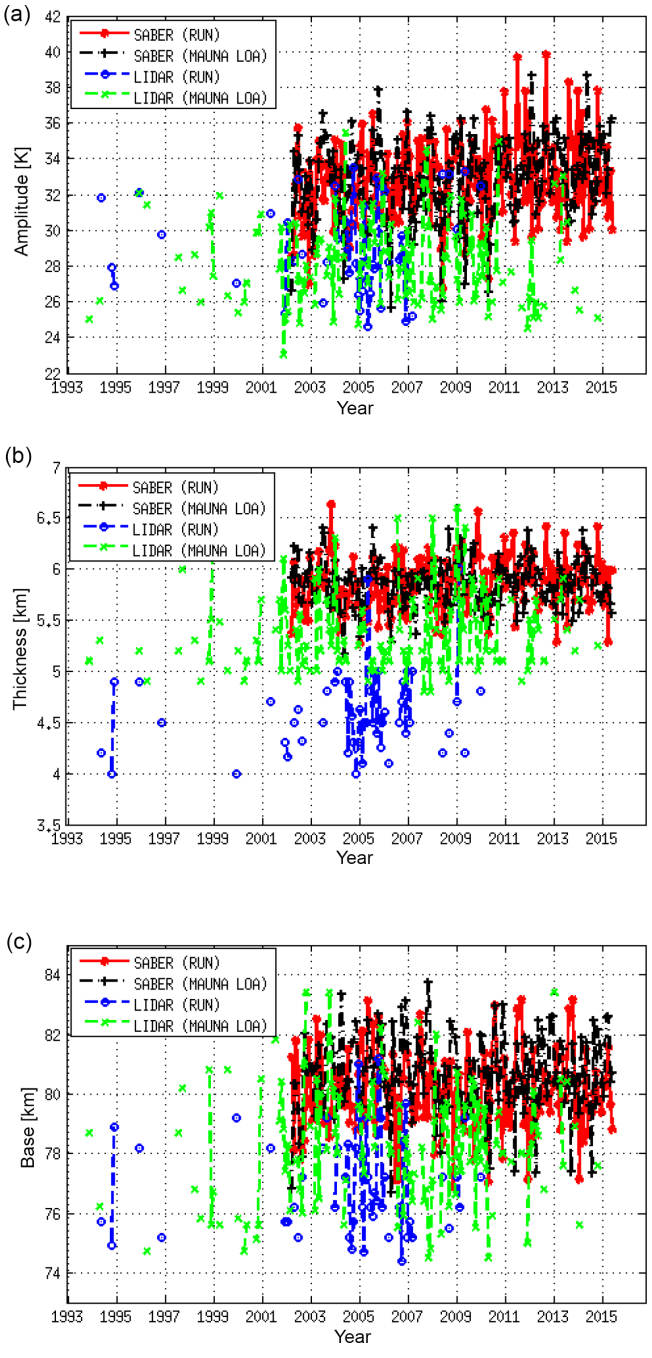

Figure 5. Time evolution of monthly **(a)** amplitude, **(b)** thickness and **(c)** base of the inversion layer obtained from lidar and SABER observations over Réunion and Mauna Loa, respectively, for the period 1993–2014.

5 Discussion

5.1 Characteristics of the MILs

Our results reveal the existence of similarities in the characteristics of the MILs (amplitude, thickness, base) over these two quasi-symmetrical tropical sites. The characteristics of the MILs over these sites seem to be dominated by the semi-annual cycle with maximum and minimum observed near equinoxes and solstices, respectively. The semi-annual cycle is clearly observed from both lidar and SABER temperature profiles over both sites. These similarities in the evolution of MILs at Réunion and Mauna Loa confirm the results of Gan et al. (2012) obtained on a global scale. Based on SABER observations from 2002 to 2009, Gan et al. (2012) showed the global distribution of the monthly zonal mean occurrence rate and the characteristics of MILs. They found in both hemispheres that the evolution of the characteristics of MILs followed a semi-annual cycle at low latitudes and an annual cycle at mid-latitudes. Previously, Leblanc and Hauchecorne (1997) used HALOE observations to show the existence of a strong semi-annual cycle on the evolution of MIL characteristics in a lower latitude belt centred on the Equator and covering the tropical region. According to these global studies, observations are therefore expected to show a semi-annual cycle on the evolution of MIL characteristics over two tropical sites that are symmetrically located with respect to the Equator such as Réunion and Mauna Loa. In agreement with previous research, results presented in this study also confirm the fact that the latitudinal variations in the characteristics of the MILs are symmetrical with respect to the Equator. Although the differences between Réunion and Mauna Loa are statistically significant, it is noted that the mean values are roughly close, particularly according to SABER observations (see Fig. 4). This study reveals that the MILs at Réunion appear on average thinner (∼ 1 km), lower (∼ 1 km) but with a higher amplitude (∼ 2 K) than Mauna Loa. Apart from amplitude, the difference in MILs between Réunion and Mauna Loa are consistent with the work of Gan et al. (2012). To summarize, the present results indicate that MILs in the Southern Hemisphere usually appear to be thinner, lower and with a larger amplitude than those observed in the Northern Hemisphere.

Moreover, by analysing HALOE observations from 1991 to 2001, Fadnavis and Beig (2004) found a strong semi-annual cycle in the evolution of the MILs over the north Indian tropical region (0–30° N, 60–100° E). In this study, excluding amplitude, it is noted that the base and the thickness variations obtained at Réunion and Mauna Loa compare fairly well with their results over the north of the Indian tropical region. Indeed, they found that the monthly mean amplitude varies from 7 to 12 K, whereas at Réunion the monthly mean amplitude varies from 29 to 33 K and from 28 to 36 K according to lidar and SABER observations, respectively. It should be noted that the monthly mean amplitude variations obtained by Fadnavis and Beig (2004) are also weak in comparison to the amplitude obtain at Mauna Loa in this investigation. The statistical analysis completed by Fechine et al. (2008) over an Atlantic tropical region (17° S–3° N, 26–40° W) provides a better comparison with the results presented here. Using SABER observations during 2005, Fechine et al. (2008) obtained monthly mean amplitude evo-

lution similar to the results presented here but with values ranging from 17 to 34 K. It should also be noted that the monthly mean thickness and base variations shown in Fig. 4 are in agreement with the work of Fechine et al. (2008). Furthermore, the amplitude variations observed by Ratnam et al. (2003) from lidar observations over an Indian tropical site are in fairly good agreement with this study. Based on about 40 months of lidar data measured from 1998 to 2003 over Gadanki (13.5° N, 79.2° E), Ratnam et al. (2003) observed monthly mean amplitude ranging from 16 to 33 K with the peak occurring mostly during equinoxes. Moreover, they found that the evolution of the characteristics of MILs follows an annual cycle over tropical regions. This result is in disagreement with the results presented in this study and those usually observed over tropical regions. It is worth noting that, using lidar observations at Gadanki from 1998 to 2007, Kishore Kumar et al. (2008) found a clear semi-annual cycle in MIL occurrence.

In general, the statistical results for the two tropical regions presented in this investigation are in fairly good agreement with previous studies (Leblanc and Hauchecorne, 1997; Siva Kumar et al., 2001; Fadnavis and Beig, 2004; Meriwether and Gerrard, 2004; Fechine et al., 2008; Gan et al., 2012). Most previously reported studies on MIL occurrences over tropics are based on satellite observations. As a consequence, the discrepancies existing between results presented in this study and previous investigations could be mainly due to different measurement techniques or horizontal resolution observation. Unlike satellite experiments that allow global observations, a ground-based lidar system is able to derive temperature profiles at a specific location.

5.2 SABER and lidar observations: effects of spatial coincidences

In the present study, the monthly mean characteristics of MILs obtained from SABER satellite observations are on average greater than those obtained by lidar systems operating at Réunion and Mauna Loa. Figure 6 depicts the monthly mean and standard deviations of the differences between lidar and SABER observations on both sites. The difference in amplitude is about 5 K during the boreal spring months (March–April) and boreal autumn months (August and October) at Mauna Loa (Fig. 6a). Except during the boreal winter months (January–February) and April, the difference in amplitude is ranging from 0.5 to 2 K at Réunion. In contrast to amplitude, the difference in thickness at Réunion (average of 1.1 km) is greater than at Mauna Loa (average of 0.4 km) (Fig. 6b). At both sites, the differences in the base of temperature inversion reach their maximum value (2 km) during the spring months (March–May) and decrease below 1 km during the autumn months (September–October) (Fig. 6c). These discrepancies are probably due to several factors such as horizontal resolution, instrument noise and probably tidal variability. Morel et al. (2002) studied the

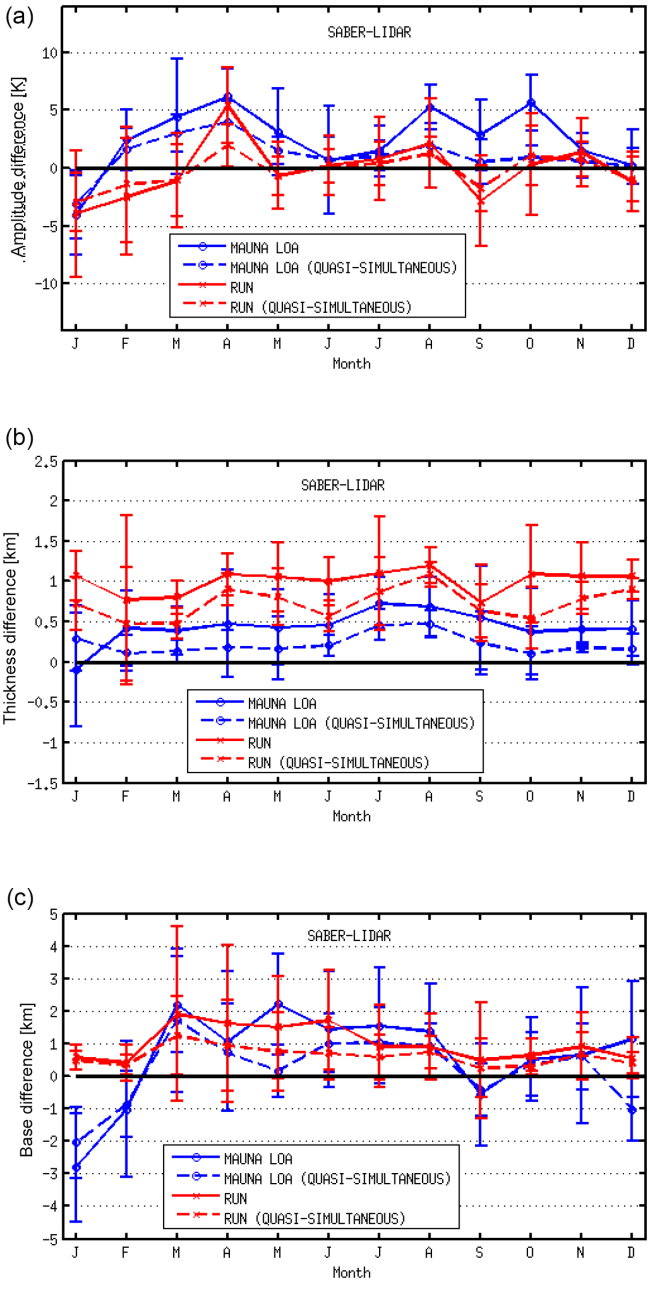

Figure 6. Mean monthly difference and standard deviation of **(a)** amplitude, **(b)** thickness and **(c)** base of the inversion between lidar and nearest SABER coincidences (dashed line) and whole SABER observations (solid line) over Mauna Loa during 2002–2014 (blue line) and over Réunion during 2002–2009 (red line).

tidal perturbations in the temperature profile measured by the Rayleigh lidar at Réunion. Based on a limited dataset (2–3 weeks during November 1995), they found the presence of a tidal component with downward phase propagation, specifically a warmer early night and a colder midnight in the stratosphere and the lower mesosphere. Comparison between SABER and lidar observations have also

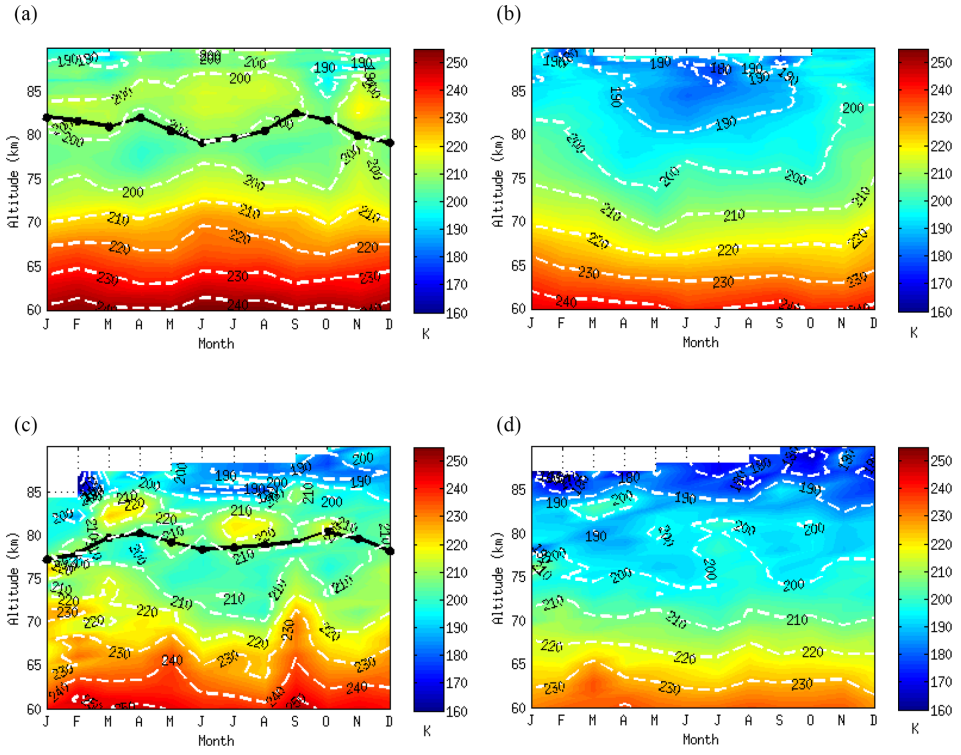

Figure 7. Mean monthly temperature profiles with **(a, c)** and without **(b, d)** inversion layer over Mauna Loa **(a, b)** and Réunion **(c, d)** during 1994–2014 and 1994–2009, respectively. The black line represents the mean base of the inversion layer.

been carried out by selecting coincidences in order to reduce spatial and time dispersion between SABER and lidar profiles. For a given lidar temperature profile, the closest SABER profile in time and space is selected. According to these criteria, together with the previously criterion mentioned in Sect. 2.2, 81 and 30 lidar–SABER coincident temperature profiles were obtained at Mauna Loa and Réunion, respectively, with a spatio-temporal dispersion of $\pm 1°$ and ± 4 h. The characteristics of these lidar–SABER coincidences are given in Table 2. Figure 5 also shows the monthly mean and standard deviations of the differences between lidar and SABER coincident profiles (dashed lines). It is therefore possible to observe a reduction in the discrepancies between lidar and SABER observations. On average, a reduction of 2 K, 0.5 km and 0.7 km in amplitude, thickness and base of the temperature inversion, respectively, was obtained (see Fig. 6). When spatial and time variability adjustments are applied the discrepancies between lidar and SABER measurements are clearly reduced. Given that the estimated temperature error by SABER is between ± 1.5 and ± 2 K in the 15–80 km altitude range (Garcia-Comas et al., 2008), it can therefore be concluded that the characteristics obtained from lidar and SABER observations are in significant agreement.

5.3 Influence of the semi-annual oscillations

Figure 7 depicts the monthly mean temperature profiles with and without inversion layers at Réunion and Mauna Loa as recorded by lidar. On average, the temperature of the base of the inversion layers at Réunion is 10 K warmer than that observed at Mauna Loa (see Fig. 7a and c). Furthermore, the temperature of the MIL base at Réunion is also found to be warmer than over Cariri (7.5° S, 36.5° W), Brazil. A study by Fechine et al. (2008), which was conducted using SABER observations, indicated that the temperature at the base of the temperature inversion was approximately 205 K. Over both sites, it can be seen that the inversion layer does not necessarily occur with an accompanied cooling in the lower part (see Fig. 7a and c). At Réunion, the temperature lapse rate near the base of the inversion on February is $10\,\mathrm{K\,km^{-1}}$, whereas on June the lapse rate is $-5\,\mathrm{K\,km^{-1}}$.

Giving a detailed explanation of intra- and inter-annual variability of MILs is not an easy task because their formation mechanisms are still not well understood. It is widely accepted that the interaction between gravity waves and the mean flow is involved in the creation of these inversion layers. The breaking of gravity waves will therefore contribute a heating effect (which may be small) at the inversion locations. Given that MILs at Mauna Loa and Réunion are driven by a clear semi-annual cycle (see Figs. 2 and 4) and that temperature is characterized by a semi-annual oscillation across

Table 2. Characteristics of SABER–lidar comparisons. No temperature profiles were recorded at Réunion during 2007 because of technical problems with the Rayleigh lidar system.

Site	Number of comparisons	Average spatial separation (°)	Average time separation (hours)	Period
Mauna Loa	81	1	1–4	2002–2014
Réunion	30	1	1–4	2002–2006 2008–2009

the tropical region (Clancy et al., 1994; Ray et al., 1994; Xu et al., 2007; Ratnam et al., 2008), the possibility cannot be excluded that the formation of MILs at these sites could be induced by semi-annual oscillations in the mesospheric mean temperature. Based on SABER observations, Xu et al. (2007) suggested that the lower MILs over the equatorial region were induced by semi-annual oscillations in the mesospheric temperature. Gan et al. (2012) based their analysis on SABER observations and also suggested that MILs have semi-annual oscillations, which yield a temperature enhancement of more than 12 K over the Equator.

Figure 8 shows the normalized frequency spectrum of monthly temperature profiles recorded by lidar in the altitude range 60–90 km at Mauna Loa and Réunion. For both sites the principal peaks correspond to a quasi-semi-annual component with a frequency ranging from 0.15 to 0.17 month^{-1} (i.e. 5.8–6.6-month period), particularly over Mauna Loa. A very similar spectral decomposition is obtained for Réunion, namely the principal peak is centred at a frequency $f = 0.17$ month^{-1}. This corresponds to an oscillation with a period of approximately 5.8 months and could be associated with the semi-annual cycle (Fig. 8b). In addition, both spectrums obtained for Réunion and Mauna Loa reveal a second peak at about 0.08–0.10 month^{-1} (corresponding to a period of 10–12 months). This can be associated with seasonal annual forcing. It should be noted that the altitude range of these two oscillations is different at the two sites. The annual oscillation is observed at an altitude between 62 and 90 km at Réunion, whereas it appears between 60 and 75 km at Mauna Loa. A significant observation is also that the magnitude of the semi-annual oscillations varies with height (see Fig. 8). For both sites, the peak in magnitude (normalized value greater or equal to 0.8) appears at 74 and 84 km, which corresponds to the altitude range of the temperature inversion zone. In contrast to Réunion, a peak in magnitude of the semi-annual and annual component is also found below the temperature inversion zone at Mauna Loa.

Nevertheless, we cannot exclude the possibility of tidal aliasing which could underestimate the semi-annual oscillation influence in lidar observations (Gan et al., 2012, 2014; Xu et al., 2007). Leblanc and Hauchecorne (1997) reported that some tidal residuals can affect the altitude and amplitude of some temperature inversions. In order to reduce the

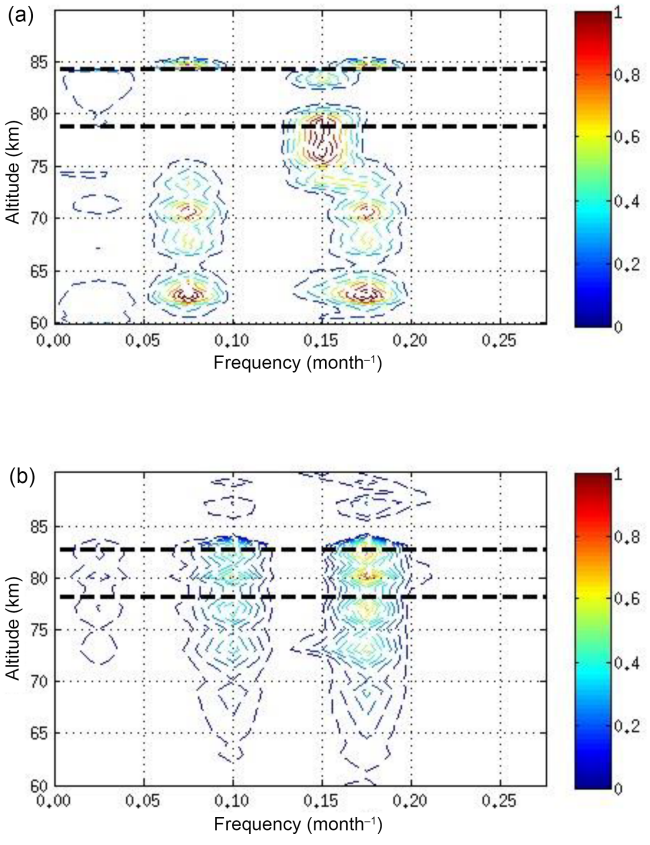

Figure 8. Normal frequency spectrum of the monthly mean temperature profiles obtained from lidar observation over **(a)** Mauna Loa and **(b)** Réunion. The black line indicates the temperature inversion layer.

tidal perturbation in our analysis of the semi-annual influence, we created a 60-day averaged (as SABER takes 60 days to complete a diurnal cycle over a given location) time series from the temperature profiles SABER observed within ±5° in latitudinal and longitude shift around the lidar sites, i.e. Réunion and Mauna Loa. Figure 9 illustrates the normalized frequency spectrum of the 60-day average of temperature profiles between 60 and 90 km over the two sites. At both sites, the two main detected peaks, respectively, correspond to semi-annual oscillation (with a period of approximately 5.8 months, $f = 0.17$ months^{-1}) and annual os-

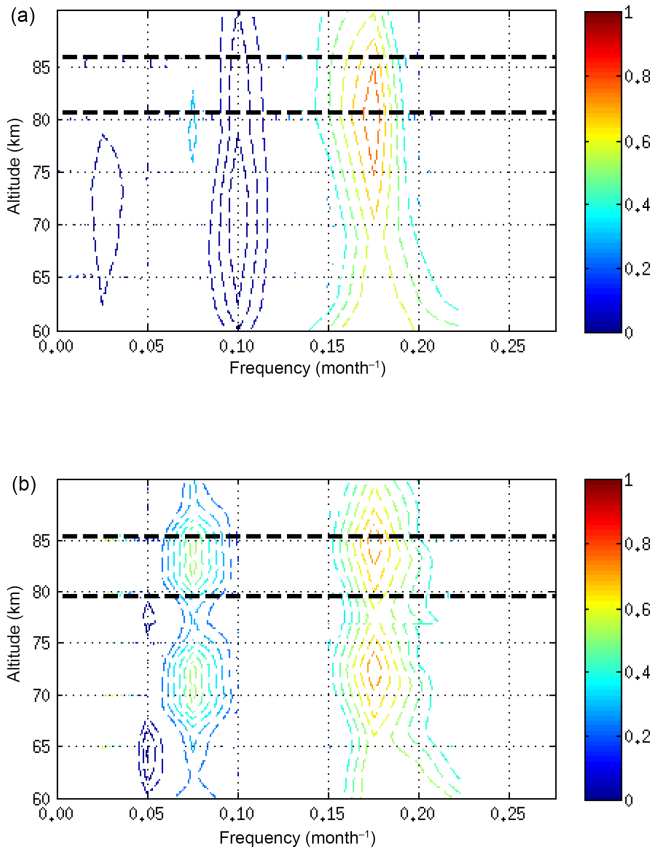

Figure 9. Normalized frequency spectrum of the 60-day averaged of temperature profile obtained from SABER observations during the 2002–2014 period over **(a)** Mauna Loa and **(b)** Réunion.

cillation (with a period of the order of 11.1–12.5 months, $f = 0.08$–0.09 months^{-1}). The spectrum's height variation obtained from SABER clearly reveals a significant variation in the magnitude of the semi-annual oscillation near to the altitude range of the temperature inversion (the altitude range 75–85 km). This connection between increase in the semi-annual component close to the inversion zone is in agreement with Gan et al. (2012). They showed a normalized frequency spectrum of the 60-day averaged zonal mean temperature observed at the Equator by SABER between 65 and 90 km. Their investigation showed that peaks of both semi-annual and annual oscillations appear at approximately 75 and 85 km. Moreover, they demonstrated that the semi-annual oscillation is the strongest between 75 and 85 km, with a maximum magnitude of 7 K. We note that this altitude range of the maximum magnitude of the semi-annual oscillation is found to be in agreement with the work presented here (Fig. 9). Moreover, based on SABER observations during the 2002–2006 period, Xu et al. (2007) showed that the amplitude of the semi-annual oscillation is larger in comparison with the annual mean temperature, which leads to MIL formation in the zonal mean temperature around the Equator at equinox. In an earlier investigation, Shepherd et al. (2004) applied a Lomb–Scargle normalized periodogram to the temperature measurements at all latitudes obtained by the WIND Imaging Interferometer (WINDII) on board UARS. In their study, they indicated that at the ±20° latitude range the semi-annual oscillations are the most dominant harmonics particularly between the altitudes of 77 and 86 km. More recently, through the use of HALOE and SABER observations, Kishore Kumar et al. (2014) investigated the long-term variations like annual, semi-annual and quasi-biennial oscillations in temperature profiles (in the altitude range 30–80 km) over Réunion during the 1992–2011 period. They also found semi-annual peak amplitude at around 75 km altitude over the Réunion site which is in agreement with the present study (Fig. 9). Using SABER observations between 2002 and 2008, Dou et al. (2009) estimated that the amplitude of the semi-annual oscillation in temperature profile in the mesosphere region is ranging from 2 to 5 K at the latitudes of Réunion and Mauna Loa sites.

It is well known that the dynamics in tropical regions are governed by an interplay of the quasi-biennial oscillation which is dominant in the lower/middle stratosphere and the semi-annual oscillation which is dominant in the upper stratosphere/lower mesosphere (Baldwin et al., 2001). It is known from the modelling and satellite studies that the quasi-biennial oscillation and the semi-annual oscillation have their origin in the gravity waves mainly generated in the troposphere (Mayr et al., 1999; Ern et al., 2015). The results obtained in the present paper reveal a weak peak in magnitude ranging from 0.03 to 0.04 month^{-1} (corresponding to a period of 25–33 months), which could be associated with quasi-biennial oscillation (Figs. 8 and 9). At both sites, this peak is associated with a normalized value less than or equal to 0.1. This result is found to be in agreement with Shepherd et al. (2004). Based on a Lomb–Scargle normalized periodogram on the WINDII observations during the 1991–1997 period, they obtained for the quasi-biennial oscillation a magnitude weaker than the magnitude obtained for the semi-annual oscillation at the altitude range of the temperature inversion zone. Through the use of satellite observations over Réunion site, Kishore et al. (2014) revealed that quasi-biennial oscillation amplitudes at 26 and 30 months show smaller magnitude than semi-annual oscillation in the mesosphere. There are a few studies showing the relationship between the mesospheric semi-annual oscillation and the stratospheric quasi-biennial oscillation (Burrage et al., 1996; Sridharan et al., 2007; Ratnam et al., 2008; Kishore Kumar et al., 2014). In general, the magnitude of the mesospheric semi-annual oscillation observed between 72 and 78 km is strongly modulated by phase of the stratospheric quasi-biennial oscillation. Based on mesospheric zonal wind observations from 1977 to 2006, Ratnam et al. (2008) showed that the modulation is apparent in this altitude range during the mesospheric semi-annual oscillation westward phase, which is considerably stronger when

the stratospheric quasi-biennial oscillation winds are mainly eastward.

6 Summary and conclusion

A statistical analysis of the characteristics of the MILs for two tropical locations has been presented in this investigation. The analysis focused on Réunion (20.8° S, 55.5° E) and Mauna Loa (19.5° N, 155.6° W). These locations were selected because of their symmetrical position with respect to the Equator together with the availability of ground-based lidar data. This study employed 16 and 21 years of lidar observations recorded at Réunion and Mauna Loa, respectively, in association with SABER observations. The occurrence rate of MILs calculated from ground-based and satellite observations appears slightly higher at Réunion when compared to Mauna Loa. The frequency of occurrence of MILs calculated from lidar observations is 10 and 9.3 % at Réunion and Mauna Loa, respectively. Over Réunion, a peak in MIL occurrence is observed in January. This is 2 times higher when compared to Mauna Loa observations. This peak in MIL occurrence could be linked to the presence of tropical cyclones, which are known to be the source of low-frequency convective gravity waves over the SWIO. Analysis of the PDFs shows that the characteristics (amplitude, thickness, base) of MILs are distributed following a normal law. At both sites, the temperature inversion zone is found on average to be in the altitude range 75 to 86 km with a maximum amplitude exceeding 30 K. Furthermore, the results obtained from lidar and SABER observations are in fairly good agreement. The results presented in this study compare reasonably well to previous studies carried out in tropical regions. When compared with Réunion, the temperature of the base of MILs is on average 10 K weaker at Mauna Loa. The MILs at Réunion appear on average thinner ($\sim$ 1 km), lower ($\sim$ 1 km) and with a higher amplitude ($\sim$ 2 K) than Mauna Loa. The confidence intervals of the mean calculated at 95 % reveal that the differences between these two sites are statistically significant. Although the differences are statistically significant, it can be seen that the mean thickness and base values are still relatively close.

The frequency of occurrence and the characteristics of the MILs at both sites evolve in time following a semi-annual cycle with maximum and minimum observed near the equinoxes and solstices, respectively. The presence of a semi-annual cycle on the characteristics of the MILs is found to be in agreement with previous studies using satellites observations over tropical locations. In this investigation, frequency spectrum analysis of temperature profiles from lidar and SABER reveals the presence of significant semi-annual oscillation, where the maximum magnitude coincides with the height range of the temperature inversion zone. These results suggest a contribution of the semi-annual oscillation to the formation of MILs at the two tropical sites. Moreover, this contribution could be modulated by the stratospheric quasi-biennial oscillation mainly during its eastward phase. Given that the semi-annual oscillation could contribute approximately 30 % to the maximum amplitude of MILs over the Equator (Gan et al., 2012), we cannot exclude the possibility of a generation mechanism based on a coupling of the semi-annual oscillation and other processes, such as chemical heating and wave breaking. The contribution of semi-annual oscillations and the role of other contributing factors affecting the formation mechanism of MILs at these tropical sites therefore require further investigation and will form the basis for a forthcoming study.

Data availability. The data used for this study are produced and available on the NDACC website (http://www.ndsc.ncep.noaa.gov/) and on the SABER website (http://saber.gats-inc.com).

Competing interests. The authors declare that they have no conflict of interest.

Acknowledgements. This work is undertaken within the framework of the International Research Group GDRI ARSAIO (Atmospheric Research in Southern Africa and Indian Ocean; research project UID number: 78682) and the STIC (Stratosphere-Troposphere Interactions and Change) project, supported by the French–South African PHC/Protea programme. The authors also thank the NDACC network for providing the lidar data for this study (http://www.ndsc.ncep.noaa.gov/). The authors would like to thank the members of the JPL and OPAR for the lidar measurements at Mauna Loa and Réunion, respectively. The authors would especially like to thank the staff of the team working on the SABER measurements (http://saber.gats-inc.com/data.php). We thank Barbara Lynn Duigan (National Astrophysics and Space Science programme at University of KwaZulu Natal and Atmospheric Research group at School of Chemistry and Physics at University of KwaZulu Natal) for her contribution to improve the English of the manuscript.

The topical editor, Christoph Jacobi, thanks Kishore Kumar Grandhi and one anonymous referee for help in evaluating this paper.

References

Baldwin, M. P., Gray, L. J., Dunkerton, T. J., Hamilton, K., Haynes, P. H., Randel, W. J., and Jones, D. B. A : The quasi-biennial oscillation, Rev. Geophys., 39, 179–229, 2001.

Barnett, J. J. and Corney, M.: Middle atmosphere reference model derived from satellite data, Middle Atmosphere Program, in: International Council of Scientific Unions Middle Atmosphere Program, Handbook for MAP, 16, 86–137, 1985.

Batista, P. P., Clemesha, B. R., and Simonich, D. M.: A 14-year monthly climatology and trend in the 35–65 km altitude range from Rayleigh LIDAR temperature measurements at a low latitude station, J. Atmos. Sol.-Terr. Phy., 71, 1456–1462, 2009.

Bencherif, H., Keckhut, P., Hauchecorne, A., Leveau, J., Megie, G., and Bessa, M.: Rayleigh-Mie Lidar measurements over Reunion Island: Validation and preliminary results, 18th International Laser Radar Conference, Berlin, Germany, 1996.

Bencherif, H., Charyul, D. V., Amraoui, L. E., Peuch, V.-H., Semane, N., and Hauchecorne, A.: Examination of the 2002 major warming in the Southern Hemisphere using ground-based and Odin/SMR assimilated data: stratospheric ozone distribution and tropic/mid-latitude exchange, Can. J. Phys., 85, 1287–1300, 2007.

Berger, U. and von Zahn, U.: The two-level structure of the mesopause: a model study, J. Geophys. Res., 104, 22083–22093, 1999.

Burrage, M. D., Vincent, R. A., Mayr, H. G., Skinner, W. R., Arnold, N. F., and Hays, P. B.: Long-term variability of the equatorial middle atmosphere zonal wind, J. Geophys. Res., 101, 12847–12854, 1996.

Cadet, B., Goldfarb, L., Faduilhe, D., Baldy, S., Giraud, V., Keckhut, P., and Réchou, A.: A sub-tropical cirrus clouds climatology from Reunion Island (21° S, 55° E) lidar data set, Geophys. Res. Lett., 30, 1130, https://doi.org/10.1029/2002GL016342, 2003.

Chanin, M. L. and Hauchecorne, A.: Lidar studies of temperature and density using Rayleigh scattering, MAP Handbook, 113, SCOSTEP, Urbana, IL, USA, 87–98, 1984.

Chane-Ming, F., Faduilhe, D., and Leveau, J.: Latitudinal and seasonal variability of gravity-wave energy in the South-West Indian Ocean, Ann. Geophys., 25, 2479–2485, https://doi.org/10.5194/angeo-25-2479-2007, 2007.

Chane Ming, F., Chen, Z., and Roux, F.: Analysis of gravity-waves produced by intense tropical cyclones, Ann. Geophys., 28, 531–547, https://doi.org/10.5194/angeo-28-531-2010, 2010.

Clancy, R. T. and Rusch, D. W.: Climatology and trends of mesospheric (58–90 km) temperatures based upon 1982–1986 SME limb scattering profiles, J. Geophys. Res., 94, 3377–3393, 1989.

Clancy, R. T., Rusch, D. W., and Callan, M. T.: Temperature minima in the average thermal structure of the middle mesosphere (70–80 km) from analysis of 40-to-92-km SME global temperature profiles, J. Geophys. Res., 99, 19001–19020, https://doi.org/10.1029/94JD01681, 1994.

Cutler, L. J., Collins, R. L., Mizutani, K., and Itabe, T.: Rayleigh lidar observations of mesospheric inversion layers at Poker Flat, Alaska (65° N, 14° W), Geophys. Res. Lett., 28, 1467–1470, https://doi.org/10.1029/2000GL012535, 2001.

Dao, P. D., Farley, R., Tao, X., and Gardner, C. S.: Lidar observations of the temperature profile between 25 and 103 km: evidence of tidal perturbation, Geophys. Res. Lett., 22, 2825–2828, 1995.

Dawdy, A. J., Vincent, R. A., Murphy, D. J., Tsutsumi, M., Riggin, D. M., and Jarvis, M. J.: The large-scale dynamics of the mesosphere lower thermosphere during the Southern Hemisphere stratospheric warming of 2002, Geophys. Res. Lett., 31, L14102, https://doi.org/10.1029/2004GL020282, 2004.

Dewan, E. M. and Picard, R. H.: On the origin of mesospheric bores, J. Geophys. Res., 106, 2921–2927, https://doi.org/10.1029/2000JD900697, 2001.

Dou, X., Li, T., Xu, J., Liu, H. L., Xue, X., Wang, S., Leblanc, T., McDermid, I. S., Hauchecorne, A., Keckhut, P., Bencherif, H., Heinselman, C., Steinbrecht, W., Mlynczak, M. G., and Russell III, J. M.: Seasonal oscillations of middle atmosphere temperature observed by Rayleigh lidars and their comparisons with TIMED/SABER observations, J. Geophys. Res., 114, D20103, https://doi.org/10.1029/2008JD011654, 2009.

Duck, T. J. and Greene, M. D.: High Arctic observations of mesospheric inversion layers, Geophys. Res. Lett., 31, L02105, https://doi.org/10.1029/2003GL018481, 2004.

Duck, T. J., Sipler, D. P., and Salah, J. E.: Rayleigh lidar observations of a mesospheric inversion layer during night and day, Geophys. Res. Lett., 28, 3597–3600, 2001.

Ern, M., Preusse, P., and Riese, M.: Driving of the SAO by gravity waves as observed from satellite, Ann. Geophys., 33, 483–504, https://doi.org/10.5194/angeo-33-483-2015, 2015.

Fadnavis, S. and Beig, G.: Mesospheric temperature inversions over the Indian tropical region, Ann. Geophys., 22, 3375–3382, https://doi.org/10.5194/angeo-22-3375-2004, 2004.

Fechine, J., Wrasse, C. M., Takahashi, H., Mlynczak, M. G., and Russell, J. M.: Lower-mesospheric inversion layers over Brazilian equatorial region using TIMED/SABER temperature profiles, Adv. Space Res., 41, 1447–1453, https://doi.org/10.1016/j.asr.2007.04.070, 2008.

France, J. A., Harvey, V. L., Randall, C. E., Collins, R. L., Smith, A. K., Peck, E. D., and Fang, X.: A climatology of planetary wave-driven mesospheric inversion layers in the extratropical winter, J. Geophys. Res.-Atmos., 120, 399–413, https://doi.org/10.1002/2014JD022244, 2015.

Fritts, D. and Alexander, M. J.: Gravity wave dynamics and effects in the middle atmosphere, Rev. Geophys., 41, 1003, https://doi.org/10.1029/2001RG000106, 2003.

Fritts, D. and van Zandt, T.: Spectral estimates of gravity wave energy and momentum Kuxes: energy dissipation, acceleration, and constraints, J. Atmos. Sci., 50, 3685–3694, 1993.

Gan, Q., Zhang, S. D., and Yi, F.: TIMED/SABER observations of lower mesospheric inversion layers at low and middle latitudes, J. Geophys. Res., 117, D07109, https://doi.org/10.1029/2012JD017455, 2012.

Gan, Q., Du, J., Ward, W. E., Beagley, S. R., Fomichev, V. I., and Zhang, S.: Earth Planets Space, 66, 103, https://doi.org/10.1186/1880-5981-66-103, 2014.

Garcia-Comas, M., López-Puertas, M., Marshall, B. T., Wintersteiner, P. P., Funke, B., Bermejo-Pantaleón, D., Mertens, C. J., Remsberg, E. E., Gordley, L. L., Mlynczak, M. G., and Russell III, J. M.: Errors in Sounding of the Atmosphere using Broadband Emission Radiometry (SABER) kinetic temperature caused by non-local-thermodynamic-equilibrium model parameters, J. Geophys. Res., 113, D24106, https://doi.org/10.1029/2008JD010105, 2008.

Hauchecorne, A., Chanin, M. L., and Wilson, R.: Mesospheric temperature inversion and gravity wave breaking, Geophys. Res. Lett., 14, 933–936, https://doi.org/10.1029/GL014i009p00933, 1987.

Hauchecorne, A., Keckhut, P., and Chanin, M. L.: Dynamics and transport in the middle atmosphere using remote sensing techniques from ground and space, in: Infrasound Monitoring for Atmospheric Studies, 665–683, Springer, the Netherlands, 2010.

Hedin, A. E.: Extension of the MSIS thermosphere model into the middle and lower atmosphere, J. Geophys. Res., 96, 1159–1172, 1991.

Hoffmann, P., Singera, W., Keuera, D., Hockingb, W. K., Kunzec, M., and Murayamad, Y.: Latitudina and longitudinal variability of mesospheric winds and temperatures during strato-

spheric warming events, J. Atmos. Sol.-Terr. Phy., 69, 2355–2366, https://doi.org/10.1016/j.jastp.2007.06.010, 2007.

Ibrahim, C., Chane-Ming, F., Barthe, C., and Kuleshov, Y.: Diagnosis of tropical cyclone activity through gravity wave energy density in the southwest Indian Ocean, Geophys. Res. Lett., 37, L09807, https://doi.org/10.1029/2010GL042938, 2010.

Irving, B. K., Collins, R. L., Lieberman, R. S., Thurairajah, B., and Mizutani, K.: Mesospheric Inversion Layers at Chatanika, Alaska (65° N, 147° W): Rayleigh lidar observations and analysis, J. Geophys. Res.-Atmos., 119, 11235–11249, https://doi.org/10.1002/2014JD021838, 2014.

Keckhut, P., McDermid, S., Swart, D., McGee, T., GodinBeekmann, S., Adriani, A., Barnes, J., Baray, J.-L., Bencherif, H., Claude H., De Sarra, A., Fiocco, G., Hansen, G., Hauchecorne, A., Lablanc, T., Lee, C. H., Pal, S., Megie, G., Nakane, H., Neuber, R., Steinbrecht, W., and Thayer, J.: Review of ozone and temperature lidar validations performed within the framework of the Network for the Detection of Stratospheric Change, J. Environ. Monitor., 6, 721–733, 2004.

Kishore, P., Venkat Ratnam, M., Velicogna, I., Sivakumar, V., Bencherif, H., Clemesha, B. R., Simonich, D. M., Batista, P. P., and Beig, G.: Long-term trends observed in the middle atmosphere temperatures using ground based LIDARs and satellite borne measurements, Ann. Geophys., 32, 301–317, https://doi.org/10.5194/angeo-32-301-2014, 2014.

Kishore Kumar, G. K., Venkat Ratnam, M., Patra, A. K., Vijaya Bhaskara Rao, S., and Russell, J.: Mean thermal structure of the low-latitude middle atmosphere studied using Gadanki Rayleigh lidar, Rocket, and SABER/TIMED observations, J. Geophys. Res., 113, D23106, https://doi.org/10.1029/2008JD010511, 2008.

Kishore Kumar, G., Kishore Kumar, K., Singer, W., Zülicke, C., Gurubaran, S., Baumgarten, G., Ramkumar, G., Sathishkumar, S., and Rapp, M.: Mesosphere and lower thermosphere zonal wind variations over low latitudes: Relation to local stratospheric zonal winds and global circulation anomalies, J. Geophys. Res.-Atmos., 119, 5913–5927, https://doi.org/10.1002/2014JD021610, 2014.

Leblanc, T. and Hauchecorne, A.: Recent observations of mesospheric temperature inversions, J. Geophys. Res., 102, 19471–19482, https://doi.org/10.1029/97JD01445, 1997.

Leblanc, T. and McDermid, I. S.: Quasi-biennial oscillation signatures in ozone and temperature observed by lidar at Mauna Lao, Hawaii (19.5° N, 155.6° W), J. Geophys. Res., 106, 14869–14874, 2001.

Leblanc, T., Hauchecorne, A., Chanin, M., Rodgers, C., Taylor, F., and Livesey, N.: Mesospheric temperature inversions as seen by ISAMS in December 1991, Geophys. Res. Lett., 22, 1485–1488, https://doi.org/10.1029/94GL03274, 1995.

Leblanc, T., McDermid, I. S., Hauchecorne, A., and Keckhut, P.: Evaluation of optimization of lidar temperature analysis algorithms using simulated data, J. Geophys. Res., 103, 6177–6187, 1998.

Leblanc, T., McDermid, I. S., and Ortland, D. A.: Lidar observations of the middle atmospheric thermal tides and comparison with the High Resolution Doppler Imager and Global Scale Wave Model 2. October observations at Mauna Loa (19.5° N), J. Geophys. Res., 104, 11931–11938, 1999.

Leblanc, T., Sica, R. J., van Gijsel, J. A. E., Haefele, A., Payen, G., and Liberti, G.: Proposed standardized definitions for vertical resolution and uncertainty in the NDACC lidar ozone and temperature algorithms – Part 3: Temperature uncertainty budget, Atmos. Meas. Tech., 9, 4079–4101, https://doi.org/10.5194/amt-9-4079-2016, 2016a.

Leblanc, T., Sica, R. J., van Gijsel, J. A. E., Haefele, A., Payen, G., and Liberti, G.: Proposed standardized definitions for vertical resolution and uncertainty in the NDACC lidar ozone and temperature algorithms – Part 3: Temperature uncertainty budget, Atmos. Meas. Tech., 9, 4079–4101, https://doi.org/10.5194/amt-9-4079-2016, 2016b.

Li, T., Leblanc, T., and McDermid, I. S.: Interannual variations of middle atmospheric temperature as measured by the JPL lidar at Mauna Loa Observatory, Hawaii (19.5° N, 155.6° W), J. Geophys. Res., 113, D14109, https://doi.org/10.1029/2007JD009764, 2008.

Li, T., Leblanc, T., McDermid, I. S., Wu, D. L., Dou, X., and Wang, S.: Seasonal and interannual variability of gravity wave activity revealed by long-term lidar observations over Mauna Loa Observatory, Hawaii, J. Geophys. Res., 115, D13103, https://doi.org/10.1029/2009JD013586, 2010.

Liu, H.-L., Hagan, M. E., and Roble, R. G.: Local mean state changes due to gravity wave breaking modulated by the diurnal tide, J. Geophys. Res., 105, 12381–12396, 2000.

Lubken, F. J.: Seasonal variation of turbulent energy dissipation rates at high latitudes as determined by in situ measurements of neutral density Kuctuations, J. Geophys.l Res., 102, 13441–13456, 1997.

Mayr, H. G., Mengel, J. G., Reddy, C. A., Chan, K. L., and Porter, H. S.: The role of gravity waves in maintaining the QBO and SAO at equatorial latitudes, Adv. Space Res., 24, 1531–1540, 1999.

Mbatha, N., Sivakumar, V., Malinga, S. B., Bencherif, H., and Pillay, S. R.: Study on the impact of sudden stratosphere warming in the upper mesosphere-lower thermosphere regions using satellite and HF radar measurements, Atmos. Chem. Phys., 10, 3397–3404, https://doi.org/10.5194/acp-10-3397-2010, 2010.

McDermid, I. S., Walsh, T. D., Deslis, A., and White, M. L.: Optical systems design for a stratospheric lidar system, Appl. Optics, 34, 6201–6210, 1995.

Meriwether, J. W. and Gardner, C. S.: A review of the mesosphere inversion layer phenomenon, J. Geophys. Res., 105, 12405–12416, 2000.

Meriwether, J. W. and Gerrard, A. J.: Mesosphere inversion layers and stratosphere temperature enhancements, Rev. Geophys., 42, RG3003, https://doi.org/10.1029/2003RG000133, 2004.

Meriwether, J. W. and Mlynczak, M. G.: Is chemical heating a major cause of the mesosphere inversion layer?, J. Geophys. Res., 100, 1379–1387, https://doi.org/10.1029/94JD01736, 1995.

Meriwether, J. W., Gao, X., Wickwar, V., Wilkerson, T., Beissner, K., Collins, S., and Hagan, M.: Observed coupling of the mesospheric inversion layer to the thermal tidal structure, Geophys. Res. Lett., 25, 1479–1482, 1998.

Mertens, J. C., Schmidlin, F., Goldberg, R. A., Remsberg, E. W., Pesnell, D., Russell III, J., Mlynczak, M., López-Puertas, M., Wintersteiner, P., Picard, R., Winick, J., and Gordley, L.: SABER observations of mesospheric temperatures and comparisons with falling sphere measurements taken during the 2002

summer MaCWAVE campaign, Geophys. Res. Lett., 31, L03105, https://doi.org/10.1029/2003GL018605, 2004.

Morel, B., Bencherif, H., Keckhut, P., Baldy, S., and Hauchecorne, A.: Evidence of tidal perturbations in the middle atmosphere over Southern Tropics as deduced from LIDAR data analysis, J. Atmos. Sol.-Terr. Phy., 64, 1979–1988, 2002.

Moorgawa, A., Bencherif, H., Michaelis, M. M., Porteneuve, J., and Malinga, S.: The Durban atmospheric LIDAR, Opt. Laser Technol., 39, 306–312, 2007.

Nee, J. B., Thulasiraman, S., Chen, W. N., Ratnam, M. V., and Narayana Rao, D.: Middle atmospheric temperature structure over two tropical locations, Chung Li (25° N, 121° E) and Gadanki (13:5° N, 79:2° E), J. Atmos. Sol.-Terr. Phy., 64, 1311–1319, 2002.

Raju, U. J. P., Keckhut, P., Courcoux, Y., Marchand, M., Bekki, S., Morel, B., Bencherif, H., and Hauchecorne, A.: Nocturnal temperature changes over tropics during CAWSES-III campaign: Comparison with numerical models and satellite data, J. Atmos. Sol.-Terr. Phy., 72, 1171–1179, 2010.

Remsberg, E., Lingenfelser, G., Harvey, V. L., Grose, W., Russell III, J., Mlynczak, M., Gordley, L., and Marshall, B. T.: On the verification of the quality of SABER temperature, geopotential height, and wind fields by comparison with Met Office assimilated analyses, J. Geophys. Res., 108, 5628, https://doi.org/10.1029/2003JD003720, 2003.

Ratnam, M. V., Rao, D., Narayana Rao, T., Krishnaiah, M., Bhavani Kumar, Y., Siva Kumar, V., and Rao, P. B.: Coordinated MST Radar and Lidar observations for the study of Mesospheric structures over a tropical station, J. Atmos. Sol.-Terr. Phy., 64, 349–358, 2002.

Ratnam, M. V., Nee, J. B., Chen, W. N., Siva Kumar, V., and Rao, P. B.: Recent observations of mesospheric temperature inversions over a tropical station (13.5° N, 79.2° E), J. Atmos. Sol.-Terr. Phy., 65, 323–334, 2003.

Ratnam, M. V., Kumar, G. K., Murthy, B. V. K., Patra, A. K., Rao, V. V. M. J., Rao, S. V. B., Kumar, K. K., and Ramkumar, G.: Long-term variability of the low latitude mesospheric SAO and QBO and their relation with stratospheric QBO, Geophys. Res. Lett., 35, L21809, https://doi.org/10.1029/2008GL035390, 2008.

Ray, E. A., Holton, J. R., Fishbien, E. F., Froidevaux, L., and Walters, J. W.: The tropical semiannual oscillations in temperature and ozone as observed by the MLS, J. Atmos. Sci., 51, 3045–3052, 1994.

Rees, D., Barnett, J. J., and Labitzke, K.: COSPAR International reference atmosphere 1986 Part II: Middle atmospheric models, COSPAR, Pergamon Press, New York, 1990.

Remsberg, E., Lingenfelser, G., Harvey, L., Grose, W., Russell III, J., Mlynczak, M., Gordley, L., and Marshall, B.: On the verification of the quality of SABER temperature, geopotential height, and wind fields by comparison with Met Office assimilated analyses, Geophys. Res. Lett., 108, 4628, https://doi.org/10.1029/2003JD003720, 2003.

Russell III, J. M., Mlynczak, M. G., Gordley, L. L., Tansock, J., and Esplin, R.: An overview of the SABER experiment and preliminary calibration results, in: Proceedings of SPIE, No. 3756, p. 277, 1999.

Sassi, F., Garcia, R. R., Boville, B. A., and Liu, H.: On temperature inversions and the mesospheric surf zone, J. Geophys. Res., 107, 4380, https://doi.org/10.1029/2001JD001525, 2002.

Schmidlin, F. J.: Temperature inversions near 75 km, Geophys. Res. Lett., 3, 173–176, https://doi.org/10.1029/GL003i003p00173, 1976.

Sharma, S., Kumar, P., Jethva, C., Vaishnav, R., and Bencherif, H.: Investigations of the middle atmospheric thermal structure and oscillations over sub-tropical regions in the Northern and Southern Hemispheres, Clim. Dynam., 48, 3671–3684, 2017.

She, C. Y., Yu, J. R., and Chen, H.: Observed thermal structure of a midlatitude mesopause, Geophys. Res. Lett., 20, 567–570, 1993.

Shepherd, M. G., Evans, W. F. J., Hernandez, G., Offermann, D., and Takahashi, H.: Global variability of mesospheric temperature: Mean temperature field, J. Geophys. Res., 109, D24117, https://doi.org/10.1029/2004JD005054, 2004.

Shepherd, T. G : The middle atmosphere, J. Atmos. Sol.-Terr. Phy., 62, 1587–1601, 2000.

Shepherd, T. G : Transport in the middle atmosphere, J. Meteorol. Soc. Jpn. Ser. II, 85, 165–191, 2007.

Siva Kumar, V., Bhavani Kumar, Y., Raghunath, K., Rao, P. B., Krishnaiah, M., Mizutani, K., Aoki, T., Yasui, M., and Itabe, T.: Lidar measurements of mesospheric temperature inversion at a low latitude, Ann. Geophys., 19, 1039–1044, https://doi.org/10.5194/angeo-19-1039-2001, 2001.

Sivakumar, V., Vishnu Prasanth, P., Kishore, P., Bencherif, H., and Keckhut, P.: Rayleigh LIDAR and satellite (HALOE, SABER, CHAMP and COSMIC) measurements of stratosphere-mesosphere temperature over a southern sub-tropical site, Reunion (20.8° S; 55.5° E): climatology and comparison study, Ann. Geophys., 29, 649–662, https://doi.org/10.5194/angeo-29-649-2011, 2011.

Sridharan, S., Tsuda, T., and Gurubaran, S.: Radar observations of long-term variability of mesosphere and lower thermosphere winds over Tirunelveli (8.7° N, 77.8° E), J. Geophys. Res., 112, D23105, https://doi.org/10.1029/2007JD008669, 2007.

States, R. J. and Gardner, C. S.: Thermal structure of the mesopause region (80–105 km) at 40° N latitude. Part II: Diurnal variations, J. Atmos. Sci., 57, 78–92, 2000.

Szewczyk, A., Strelnikov, B., Rapp, M., Strelnikova, I., Baumgarten, G., Kaifler, N., Dunker, T., and Hoppe, U.-P.: Simultaneous observations of a Mesospheric Inversion Layer and turbulence during the ECOMA-2010 rocket campaign, Ann. Geophys., 31, 775–785, https://doi.org/10.5194/angeo-31-775-2013, 2013.

Whiteway, J. A., Carswell, A. I., and Ward, W. E.: Mesospheric temperature inversions with overlying nearly adiabatic lapse rate: an indication of a well-mixed turbulent layer, Geophys. Res. Lett., 22, 1201–1294, 1995.

Wilks, D. S.: Statistical Methods in the Atmospheric Sciences, Academic Press, 467 pp., 1995.

Xu, J., Smith, A. K., Yuan, W., Liu, H.-L., Wu, Q., Mlynczak, M. G., and Russell III, J. M.: Global structure and long-term variations of zonal mean temperature observed by TIMED/SABER, J. Geophys. Res., 112, D24106, https://doi.org/10.1029/2007JD008546, 2007.